

Experimental and Simulation Study on Active Vibration Control of Thin Rectangular Plate by Smart Material under Harmonic Excitation

Saif Mohammed Jawad Haider * Asst. prof. Dr. Ahmed abd Al-Hussain
Department of Mechanical Engineering, College of Engineering, University of Baghdad, Iraq
* E-mail of the corresponding author: saifhaidery@yahoo.com

Abstract

In this paper the vibration of a smart cantilever plate is being controlled. Active vibration control (AVC) methods will be used to eliminate undesired vibrations in engineering structures. Using piezoelectric smart structures for the active vibration control for actuator and sensor in engineering applications. Simulation and experimental studies on active vibration control of smart structures have been presented. The closed loop control laws are incorporated into the finite element (FE) models by using ANSYS parametric design language (APDL). The proposed procedure is tested by active control for force vibration (harmonic excitation). The active vibration suppression is achieved using proportional gain method. Experiments have been conducted to verify the closed loop simulations. Smart plate consists of aluminum plate (250 mm x 180 mm x 0.5 mm) surface bonded piezoelectric patches of MIDÉ Quick Pack QP16n transducers (45.9 mm x 20.5 mm x 0.25 mm). Experimental results are obtained by LabVIEW programs developed in the study.

Keywords: Active vibration control, piezoelectric smart structures, closed loop, finite element analysis.

1. Introduction

Active Vibration Control (AVC) was well known nowadays as an optimum technique in vibration suppression of flexible structures. Due to the complexity of the dynamics system of flexible structures, vibration control process is quite a challenge. To control the vibrations in a system, different techniques have been developed. Some of these techniques and methods use piezoelectric (PZT) materials as sensors or actuators [1]. With the development of the space technology, space structures are becoming larger and more flexible, whose modal frequencies and damping ratios are relatively low. In order to meet the high precision requirement of large space structures, the application of active control for vibration suppression becomes more and more important than ever before [2]. For most of the 20th century only passive systems could be used for vibration reduction. But that has changed in last decades. New materials introduced (PZT, PVDF, electromagnetic composites) that can act as sensors or actuators both small and effective for active methods [3].

M. Kozupa and J. Wiciak studied simulations and research results of testing of the aluminum plate with active vibration control. It is analyze and compare two ways of excitation of the test plate, various influences on its vibrations and active damping control. Vibration control of the smart structure is realized through four piezoceramic PZT actuators and one PZT sensor bonded to the plate. Simulations and numerical computations of the structure are performed in ANSYS environment [4].

T.A.Zahidi , I.Z.M.Darus used vibration control of flexible plate by classical proportional feedback gain controller method is studied, experimentally. The AVC-P controller design is implemented to a full clamped flexible plate system to evaluate its vibration attenuation performance [5].

H.Karagu, L Malgaca and H .ktem used model smart structures with piezoelectric materials product in ANSYS/Multi physics, the integration of control actions into the ANSYS solution is realized [6].

2. The Finite Element Formulation for Piezoelectric Materials

Coupled field elements which consider structural and electrical coupling are required in order to perform the FE (Finite Element) analysis of piezoelectric smart structures. The coupled field element should contain all necessary nodal degrees of freedom. The piezoelectric-FE formulation used in ANSYS. Allik & Hughes (1970) laid a foundation of the mathematical procedure of ANSYS in solving a piezoelectric material problem. They considered a linear theory of piezoelectricity. The linear theory of piezoelectricity is a theory in which the elastic, piezoelectric, and dielectric coefficients are treated as constants. Constitutive equations that ANSYS use to model piezoelectric materials [7].

$$\{T\} = [c]\{S\} - [e]\{E\} \quad (1)$$

$$\{D\} = [e]^T\{S\} - [\epsilon]\{E\} \quad (2)$$

where $\{S\}$ is strain vector, $\{T\}$ is stress vector is the electric displacement, $\{E\}$ is the electric field vector, $[e]$ are the piezoelectric matrix, $[c]$ are the Elasticity matrix at constant electric field and $[\epsilon]$ is the

dielectric matrix at constant mechanical strain. Subscripts^T denotes matrix transposition [8].

rearranged in matrix form as the following:

$$\begin{Bmatrix} \{T\} \\ \{D\} \end{Bmatrix} = \begin{bmatrix} [c] & [e] \\ [e^T] & [-\epsilon] \end{bmatrix} \begin{Bmatrix} \{S\} \\ \{-E\} \end{Bmatrix} \quad (3)$$

Therefore, ANSYS only considers these material properties for piezoelectric 3-D elements, including compliance matrix, piezoelectric coupling matrix, and permittivity matrix given in table (1):

The Elasticity matrix:

$$c = \begin{bmatrix} c_{11} & c_{12} & c_{13} & 0 & 0 & 0 \\ c_{12} & c_{22} & c_{23} & 0 & 0 & 0 \\ c_{13} & c_{23} & c_{33} & 0 & 0 & 0 \\ 0 & 0 & 0 & c_{44} & 0 & 0 \\ 0 & 0 & 0 & 0 & c_{55} & 0 \\ 0 & 0 & 0 & 0 & 0 & c_{66} \end{bmatrix}$$

compliance

The piezoelectric matrix:

$$e = \begin{bmatrix} 0 & 0 & d_{31} \\ 0 & 0 & d_{32} \\ 0 & 0 & d_{33} \\ 0 & d_{24} & 0 \\ d_{15} & 0 & 0 \\ 0 & 0 & 0 \end{bmatrix}$$

coupling

The dielectric matrix:

$$\epsilon = \begin{bmatrix} \epsilon_{11} & 0 & 0 \\ 0 & \epsilon_{22} & 0 \\ 0 & 0 & \epsilon_{33} \end{bmatrix}$$

permittivity

Table (1) Material properties of piezo-patches and aluminum plate [8].

Properties	piezoelectric	aluminum plate
Young modulus(E)	-	70 (GPa)
Density	7750 (kg/m ³)	2750 (kg/m ³)
Poisson's ratio	-	0.35
Compliance		
C ₁₁	12.1x 10 ¹⁰ (N/m ²)	
C ₂₂	12.1x 10 ¹⁰ (N/m ²)	
C ₁₂	7.54x 10 ¹⁰ (N/m ²)	
C ₁₃	7.52x 10 ¹⁰ (N/m ²)	
C ₂₃	7.52x 10 ¹⁰ (N/m ²)	
C ₃₃	11.1x 10 ¹⁰ (N/m ²)	
C ₄₄	2.11x 10 ¹⁰ (N/m ²)	
C ₅₅	2.11x 10 ¹⁰ (N/m ²)	
C ₆₆	2.26 x 10 ¹⁰ (N/m ²)	
piezoelectric coupling coefficients		
d ₃₁	-5.4 (C/m ²)	
d ₃₂	-5.4 (C/m ²)	
d ₃₃	15.8 (C/m ²)	
d ₂₄	12.3 (C/m ²)	
d ₁₅	12.3 (C/m ²)	
Permittivity		
ε ₁₁	8.11x 10 ⁻⁹ (F/m)	
ε ₂₂	8.11x 10 ⁻⁹ (F/m)	
ε ₃₃	7.35 x 10 ⁻⁹ (F/m)	

The mechanical response of piezoelectric elements can be described by the equation of motion [9]

$$\{div\{T\} + F = \rho\{\ddot{u}\} \quad (4)$$

Where T, f, ρ, and \ddot{u} are stresses, body force in unit volume, density and accelerations, respectively. On the other hand, the electrical response of piezoelectric elements can be expressed by Maxwell's equation

$$\left\{ \frac{\partial D}{\partial x} \right\} = \{0\} \quad (5)$$

Where D is the electric displacement.

the piezoelectric-FE formulation can be derived in terms of nodal quantities:

$$\begin{bmatrix} [M] & [0] \\ [0] & [0] \end{bmatrix} \begin{Bmatrix} \{\dot{u}\} \\ \{\dot{v}\} \end{Bmatrix} + \begin{bmatrix} [C] & [0] \\ [0] & [0] \end{bmatrix} \begin{Bmatrix} \{u\} \\ \{v\} \end{Bmatrix} + \begin{bmatrix} [K] & [K^e] \\ [K^e]^T & [K^d] \end{bmatrix} \begin{Bmatrix} \{u\} \\ \{v\} \end{Bmatrix} = \begin{Bmatrix} \{F\} \\ \{L\} \end{Bmatrix} \quad (6)$$

where, [M] is the mass matrix derived from density and volume, Structural damping matrix [C], vector variables u and V express structural and electrical degrees of freedom. [K] is the mechanical stiffness matrix derived from elasticity matrix, [K^e] is the piezoelectric stiffness matrix derived from piezoelectric matrix, [K^d] is the dielectric stiffness matrix derived from dielectric matrix. The variables F and L are the mechanical force vector and charge vector, respectively.

3. Closed Loop System

Proportional gain is considered in this study as the control scheme for controlling the vibration of flexible plate system. The block diagram of proportional AVC system is shown in Figure.3. In this figure, **G_a**, **G**, **G_s** and **K_p** are the transfer functions of actuator, flexible plate, sensor and controller gain respectively. Generally, the controller will try to reduce the error between the reference value and its actual value until minimum error is achieved. The effectiveness of the controller action depends on the optimum setting of its parameters or proportional gain [9].

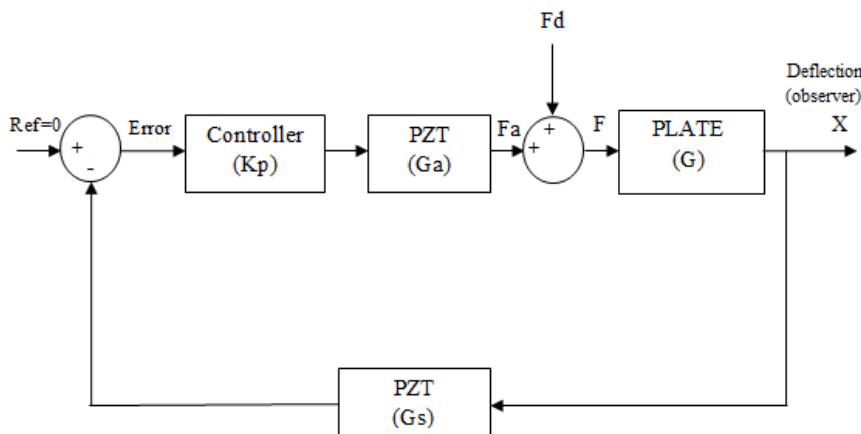


Figure 3 Block diagram of closed loop control.

For the closed loop system in Fig. 3, the reference input, which is the desired deflection, is set to zero in order to achieve zero cancellation. The input to the actuator is $-G_s K_p X$ and its output is thus $F_a = -G_a G_s K_p X$. Then the total force fed into the system is given by:

$$F = F_d + F_a = F_d - G_a G_s K_p X \quad (7)$$

Thus, the output of the system which is the deflection of the plate, **X** can be expressed as:

$$X = G F_d \left(\frac{1}{1 + G_a G_s K_p G} \right) \quad (8)$$

From equation (8), the deflection of the plate can be reduced by adjusting the controller gain, **K_p**. By increasing the controller parameter, the lateral displacement of **X** will decrease, thus suppressing the amplitude of the vibration. Theoretically, if the value of **K_p** is large, the factor $1/(1+G_a G_s K_p G)$ will tend to zero. It means that the controller can cope with any disturbance or parameter changes in the dynamics system. This type of controller is quite similar with high gain feedback regulator [10].

For the purpose of simulation, the transfer function for linear actuator and linear sensor is assumed to be unity. Thus the deflection of the plate becomes:

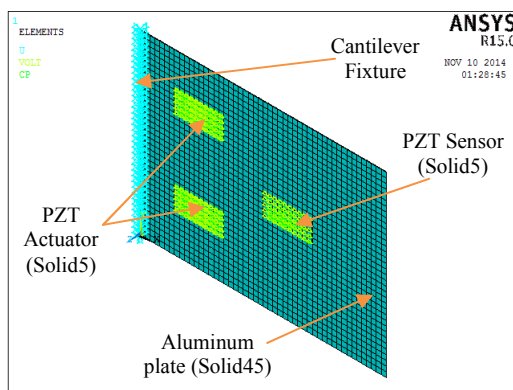
$$X = G F_d \left(\frac{1}{1 + G K_p} \right) \quad (9)$$

Based on equation (9), the deflection of the plate is inversely proportional to the value of controller gain, K_p . Thus, the amplitude of oscillation of the plate is reduced by increasing the controller gain, K_p .

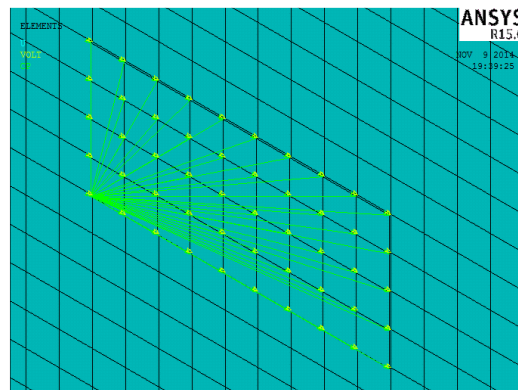
4. The FE model of Aluminum Plate and piezoelectric patch

All of the analyses are performed with script files using ANSYS parametric design language (APDL). The FE model is created using SOLID45 and SOLID5 for the aluminum plate and the piezoelectric patch respectively shown figure 4 (a)(b).

Cantilever boundary conditions are applied to the FE model. The FE model contains 1980 elements and 4226 nodes where this elements numbers are decided after a convergence study made for the ANSYS model. Natural frequencies are calculated with modal analysis by using the Block Lanczos solver. Mode shape of the smart plate corresponding to the first natural frequencies are shown in Figure (5).



(a) FEM of the cantilever plate showing



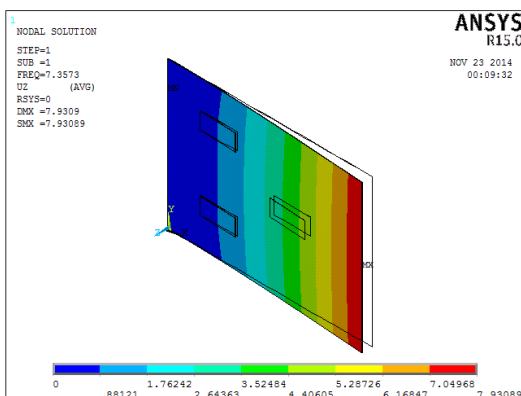
(b) Detail of the model PZT patches with electrode

Figure 4: The finite element model of the clamped cantilever plate equipped with piezoceramic patches is shown in (a), while a detailed view of the actuator and its coupled DOF is given in (b)

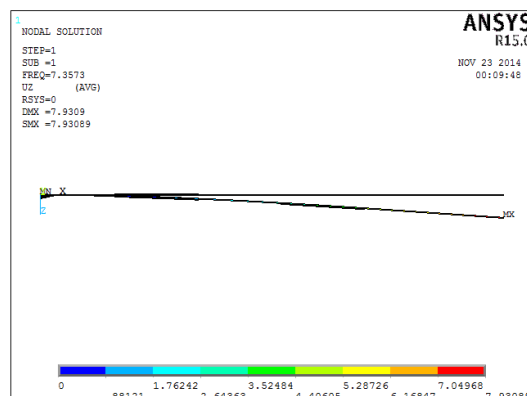
The natural frequency of the plate found with PZT and without PZT by (ANSYS program), the comparison of the natural frequencies is given in Table (2) including only the first three natural frequencies.

Table (2) illustrate natural frequency for plate with PZT and without PZT

Mode	With PZT	Without PZT	Deference (%)
1	7.3573	6.8060	%8.8
2	18.254	17.134	%6.08
3	41.806	42.131	%1.85



First Mode shape (isometric view)



First Mode shape (side view)

Figure 5 illustrates first mode shape for smart plate

5. Effect of Actuators Placement

In order to determine the influences of the actuator placement on the response, two cases are considered. At each one, by keeping the distance between the piezoelectric patches constant, the x or y position of all actuators are varied from their original configuration, and the results are given in figure 7 and 8. It is evident from the figure 8 that as the actuator are moved closer to the clamped ($x=0$) in x direction, the response increases [11]. This is due to the higher strain developed near the clamped shown figure 9.

For this reason, the patches should be placed on plate as close as possible to the clamped. Furthermore, as the patches are moved closer to the ($y=0$) edge the response remains almost unaffected [12].

For vibration control structures, the PZT is usually located continuously and discretely. Continuous collocation makes the PZT glue on the whole surface of the structure, therefore all the modes can be calculated, whereas the PZT is difficult to overspread the board especially in large aerospace structure. Discrete collocation arranges PZT on some specific Location. This method decreases the influence of PZT to the dynamic characteristics of structure but cause the problem of how to ascertain the number and location of the PZT. This study uses the D optimum design rule presented by D.S. Bayard [13]. The rule makes the optimize collocation and design of control rule as two independent processes, the best collocation of PZT is at the maximum strain of the structure. The basic thought of the rule is that response of degree of freedom is greater where the modal strain energy is higher, the actuator should be locate at the maximum strain of the structure [14]. The influence of actuator placement on the first natural frequency is also investigated and the results are shown in figure 10. It is again found that x-wise movement has greater effect.

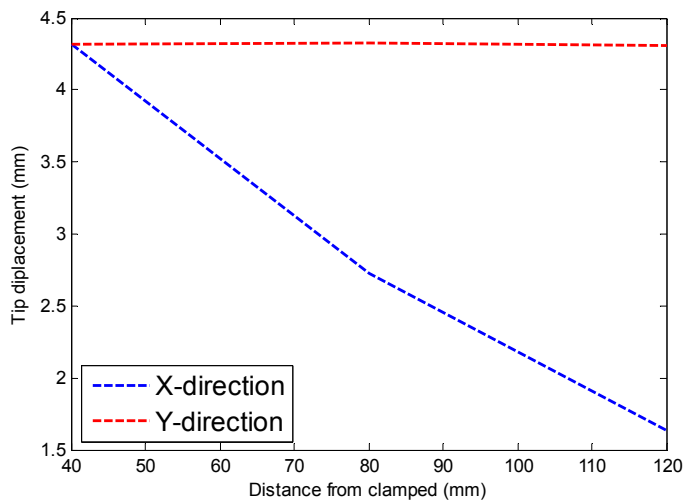
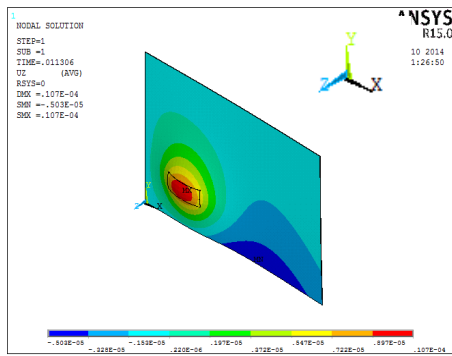
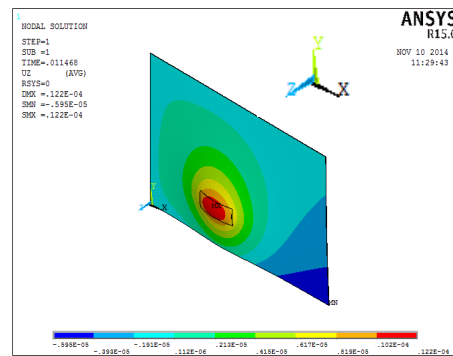


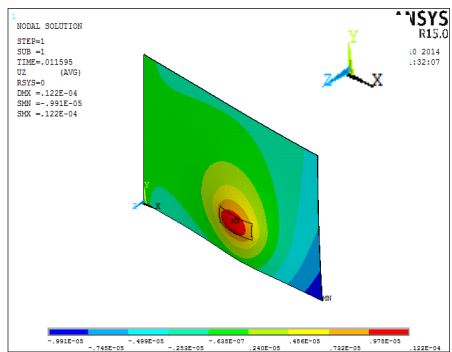
Figure 7 The influence of actuator placement on the response at 100 V (first mode)



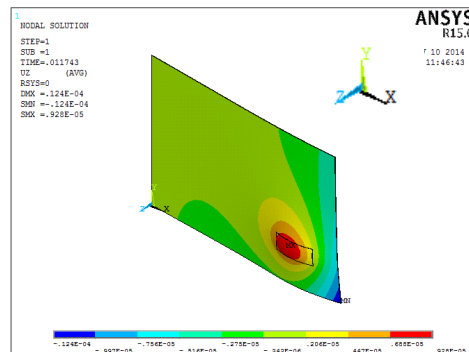
The position of actuator 40 mm from clamped



The position of actuator 80 mm from clamped



The position of actuator 120 mm from clamped



The position of actuator 160 mm from clamped

Figure 8 The influence of actuator placement on cantilever plate by ANSYS (first mode)

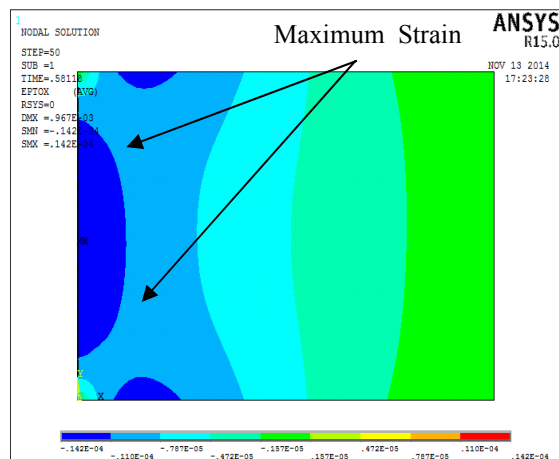


Figure 9 the total mechanical strain

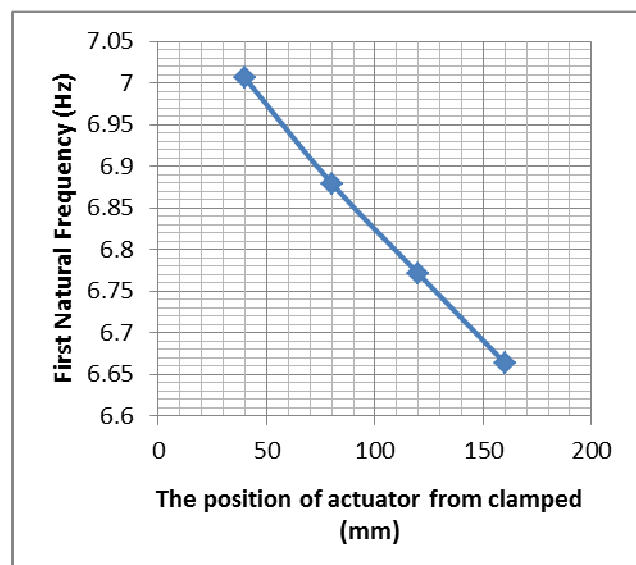


Figure 10 The influence of actuator placement on the first natural frequency of smart plate in x-direction

6. Active Vibration Control under Harmonic Excitation

In this section, the active control of a smart plate under forced vibration is analyzed. The smart plate is composed of five piezoelectric (Lead-Zirconate-Titanate) patches. three of the piezoelectric patches are used as two actuator and one sensor while the other piezoelectric patch is used as vibration generating shaker. The smart plate is harmonically excited by the piezoelectric shaker at its fundamental frequency. The PZT sensor is utilized to sense the vibration level. Active vibration reduction under harmonic excitation. Shown figure 11 illustrate of (Two PZT) shaker in the back view of plate in ANSYS

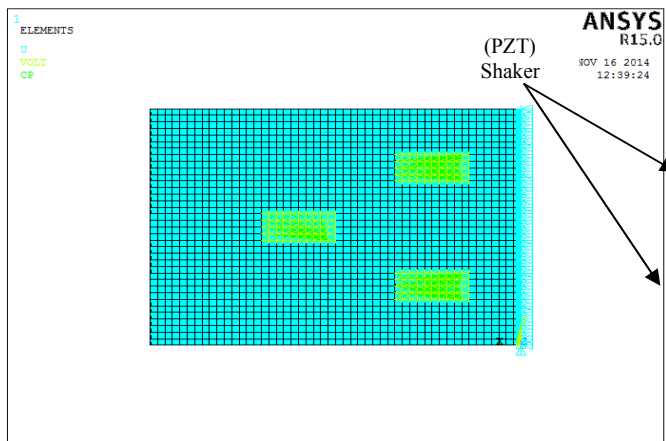


Figure 11 the FE model of Smart plate (Back view)

Active control is achieved with the integration of control actions into the FE analysis. The block diagram of the closed loop control is given in Figure 12

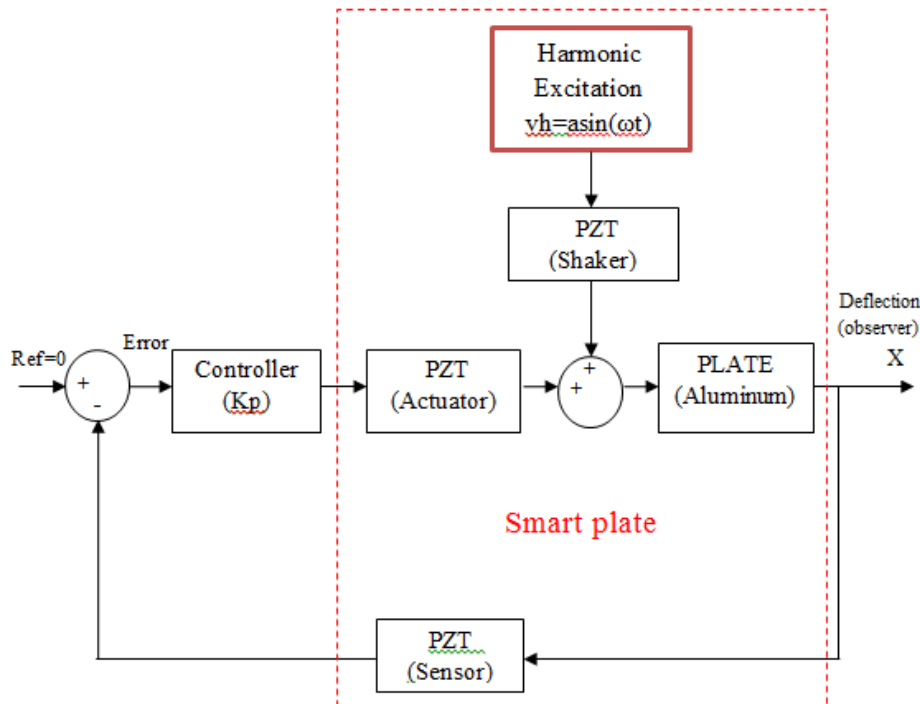


Figure 12 Block diagram of closed loop control for Harmonic Excitation.

Control actions are performed with the script code after the FE model of the smart plate is constructed. The analysis of active control is carried out by the following scripts.


```
! -----Sine.txt-----
*dim,t,,ny ! Define arrays with dimension
*dim,b,,ny
*dim,c,,ny
*dim,vh,,ny
*vfill,t(1),ramp,0,dt ! Array t(ny) : time in second
*vfact,w ! Multiplying factor: frequency=(2*pi*f1)
*vfun,b(1),copy,t(1) !Result array
b(n)=frequency*t(ny)
*vfun,c(1),sin,b(1) ! Array c(n)= sin(b(ny))
*vfact,a ! Multiplying factor: amplitude a
*vfun,vh(1),copy,c(1) ! Array vh(ny)= a*c(ny)
```

```
! Control actions
d,p5,volt,vh
d,p4,volt,vh
time,dt
solve
Ref=0
*do,i,2,ny
d,p4,volt,vh(i)
d,p5,volt,vh(i)

*get,uz,node,n,u,z
dis= ks *dis
err=Ref-ks *dis
va=kp*kv*err
d,p2,volt,va
d,p3,volt,va
time,i*dt
solve
*enddo
finish
```

Harmonic excitation is provided by the piezoelectric vibration generating shaker. The harmonic excitation $vh=asin(\omega t)$ is created with the ANSYS script “Sine.txt” as

The parameters ny , w , a are the number of samples, the circular frequency and the amplitude for the sine wave, respectively. The number of samples depends on the duration of the excitation. The excitation frequency equals to its fundamental natural frequency calculated from the modal analysis. The amplitude of the excitation is taken as 100 V due to experimental limitations. The time step is also found as $\Delta t=1/f1/20$ using the first natural frequency. The parameters b and c are temporary arrays to be able to calculate the excitation (vh). Harmonic excitation is created in the file “sine.txt” before the control loop is initiated. The first step is solved applying the excitation voltage to the piezoelectric shaker (node p4 and p5). Hence, sensor value dis in the z direction is calculated in each step after nodal displacements uz corresponding to the nodes (n) ($L=150$ mm, $W=80$ mm) in the FE model are obtained the nodal solutions of the FE model are known for the next step. Active control is realized in “*do-*enddo” loop. After sensing the actuation voltage to be applied for the piezoelectric actuator (node p2 and p3) is found multiplying error signal by the gain Kp and Kv . The analysis goes on step by step for a specific duration after vibration amplitudes reach steady-state. The parameter Kv is an amplification factor used in the experiment.

7. Experimental Work

The configuration of the smart plate including five piezoelectric patches is shown in Figure 13. The smart plate is excited by the two piezoelectric shakers at its fundamental frequency. One of the piezoelectric is used as a sensor to senses the vibration during the excitation. The other piezoelectric patch is used as an actuator to control vibrations occurred. The piezoelectric shaker is placed in the other side of PZT actuator. The plate is fixed at one end and free at the other. The dimensions of the aluminum plate and the piezoelectric are shown in Table (2).

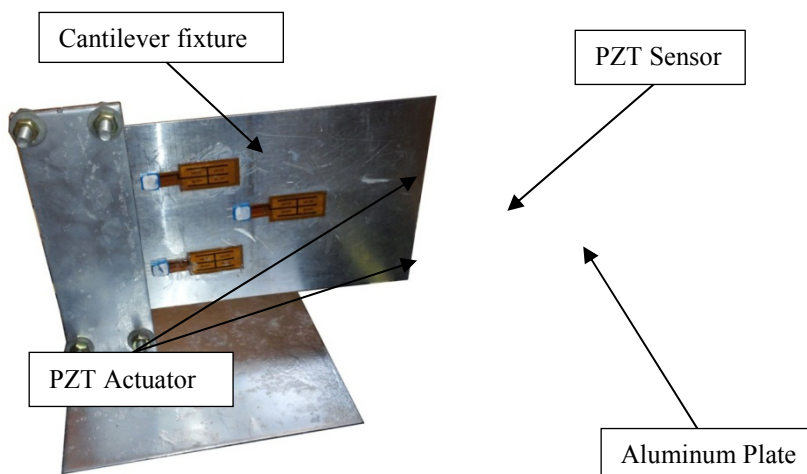


Figure 13 Cantilever plate with piezoelectric patch.

Table (2) Dimensions and location of the plate and piezoelectric

Dimensions	Plate	Piezoelectric actuator
Length	250mm	45 mm
Width	180 mm	20 mm
Thickness	0.5 mm	0.25 mm
PZT-actuator location	(40,35) mm from upper Left corner	
PZT-shaker location	(40,35) mm from upper Left corner at the other Side of plate	
PZT-sensor location	(130,80) mm from upper Left corner	

7.1 Experimental Setup

A schematic view of the experimental setup is shown in Figure 14. The Experimental setup Laboratory is shown in Figures 15. In the experimental setup, a multifunction analog input (NI 9215) and analog output (NI 9263) data acquisition (NI cDAQ-9178) chassis of NATIONAL INSTRUMENTS are utilized for data acquisition and control action.

The PZT shaker excites the plate by the sin wave signal (continuous sample) for force vibration of plate which is sent from (Laptop+ LabVIEW program), the output signal from Laptop is sent through BNC cable to analog output DAQ NI 9263 then the sin wave signal $\pm 3V$ is sent to TREK 2205 high voltage amplifier (HVPA) the gain of HVA is 32V in order to excite the piezoelectric patch about $\pm(90-100)V$. To calculated voltage range an avometer device is used, the output signal voltage from HVPA (Voltage Monitor) is sent through BNC cable to the avometer.

The PZT sensor data is acquired with the analog input DAQ NI 9215 through the input module and the signal converter from Analog to Digital by (NI cDAQ-9178) chassis then sensor data appear in (Laptop+ LabVIEW program). The input signal to the DAQ is limited by $\pm 10V$.

Later, the output signal is simultaneously sent through BNC, which is a terminal block by the analog output DAQ NI 9263 after a control signal by LabVIEW program. Then the control signal is sent to TREK 2205 high voltage amplifier (HVPA) in order to actuate the piezoelectric patch. The input signal to the HVPA is limited by ± 3 . power supply of 220 V provides necessary energy for TREK 2205 HVPA.

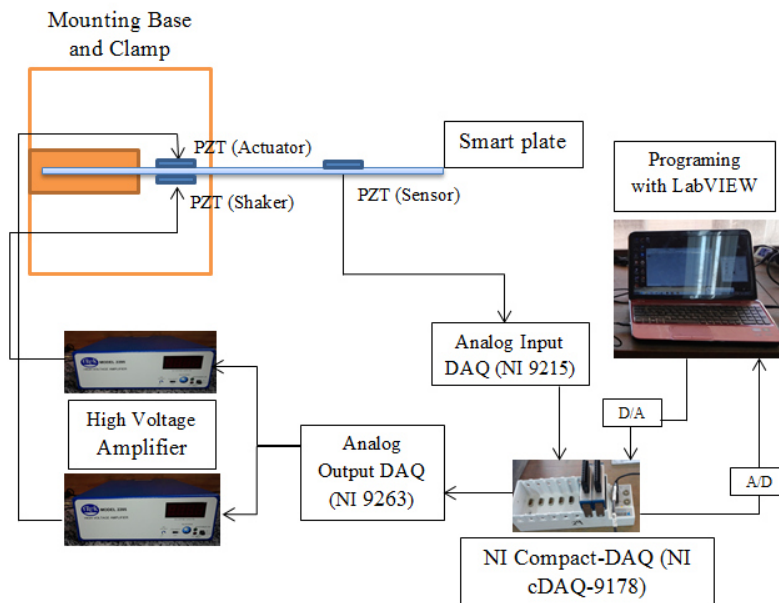


Figure (14) Schematic view of active vibration control setup.

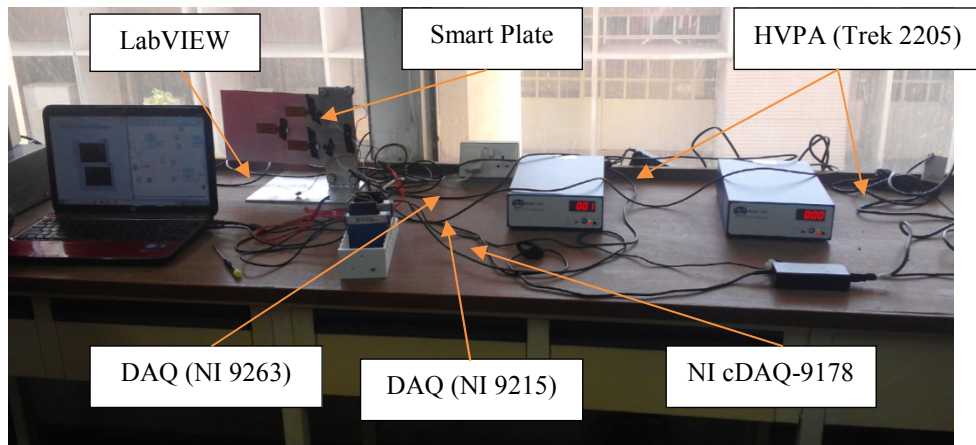


Figure (15) the experimental setup laboratory

7.2 Calibration Method:

The calibration of the PZT sensor with accelerometer is done by attaching PZT sensor on cantilever plate with known dimensions and material properties. At the free end of the cantilever plate an accelerometer is attached. Figure (16) below shows the cantilever plate with PZT sensor, accelerometer and vibrometer device.

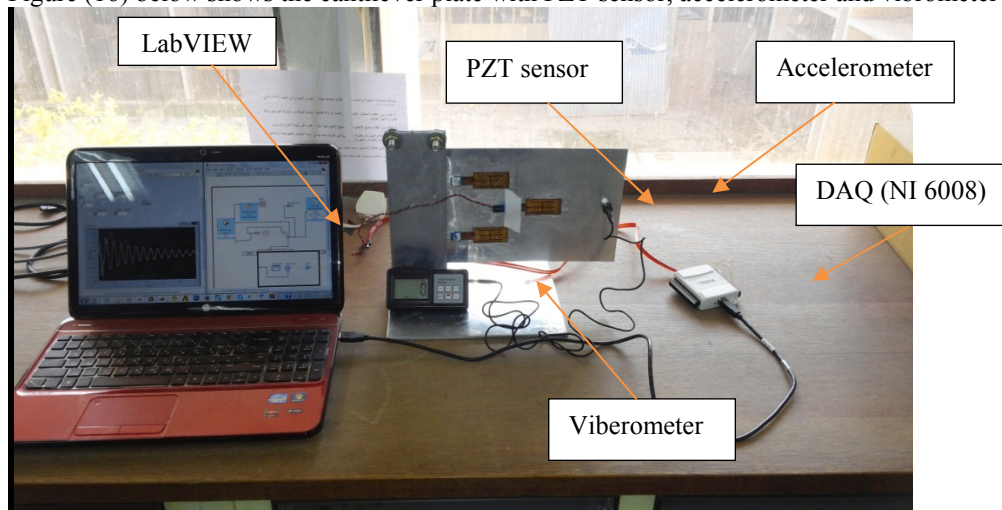


Figure (16) Calibration between displacement and voltage

The procedure of calibration is very simple where we applied random impulse on cantilever plate at free end the signal is sent to the DAQ (NI 6008) as shown in figure (16) and record the voltage by PZT sensor in LabVIEW. The Accelerometer sent the signal of deflection of plate to the vibrometer device to calculate the displacement for each impulse. Figure (17) represent the relation between the voltages and displacement. Obtained from the experimental calibration.

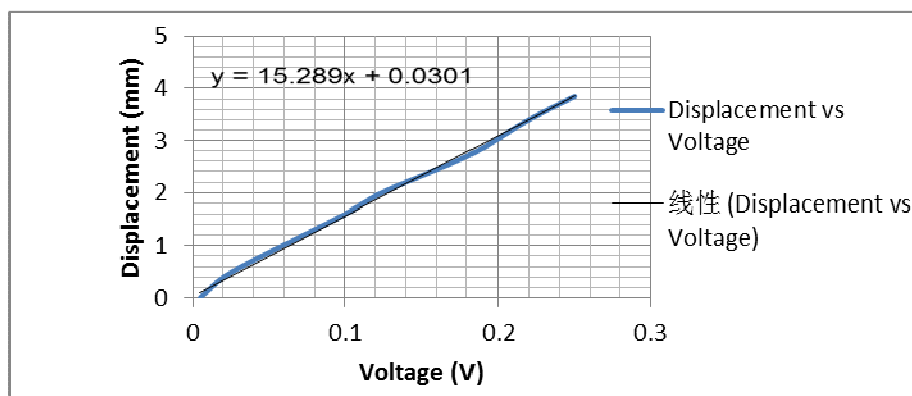


Figure (17) Displacement -Voltage curve

8. Results and Discussion

Vibration responses are obtained with both the simulation case and the experiment case. The control action is started at $t=0$ s in order to decrease steady state vibration amplitudes of the smart plate under harmonic excitation. Actuation voltages become higher if the control actions start in any time after the excitation is applied. The maximum applicable amplitude of the shaker voltage is 100 V due to the experimental limitations which the maximum control gain (K_p) is 15.

Simulation and experimental results obtained with feedback control are shown in Figures 18 ,19 for simulation case and Figures 25 ,26 for experimental case those figures include the uncontrolled and controlled responses for one and two actuator damping. The transient parts in the simulation and experiment take approximately 4 s and 3 s, respectively. The controlled responses for one and two actuator damping to reduce the amplitudes is achieved as shown in figures 18 and 19 shows a reduction of 46% for one actuator and 75% for two actuator in steady-state vibration amplitudes for simulation. Figures 25 and 26 shows a reduction of 39% and 67% in steady-state vibration amplitudes for experimental case. Reductions are close although there is a little bit amplitude difference between the simulation and experimental amplitudes. It is expected that the amplitudes obtained by the simulation are higher than those obtained by the experiment. Damping coefficients assumed in the simulation case has a pronounced effect on the vibration amplitudes. Actuation voltages are shown in figures 20-21 for one actuator damping and 22-23 for two actuator damping while the two shaker as shown in figure 24.

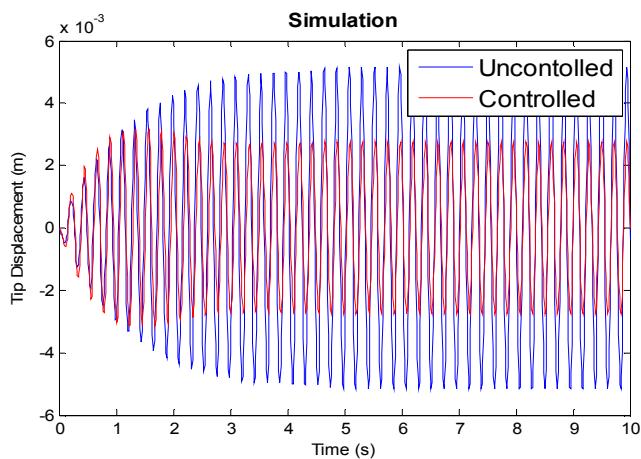


Figure 18 Uncontrolled and controlled vibration responses for one actuator damping $K_p=15$ for first mode

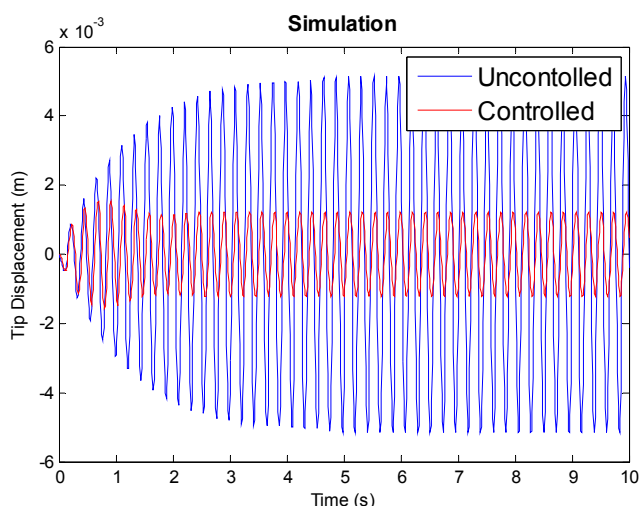


Figure 19 Uncontrolled and controlled vibration responses for two actuator damping $K_p=15$ for first mode

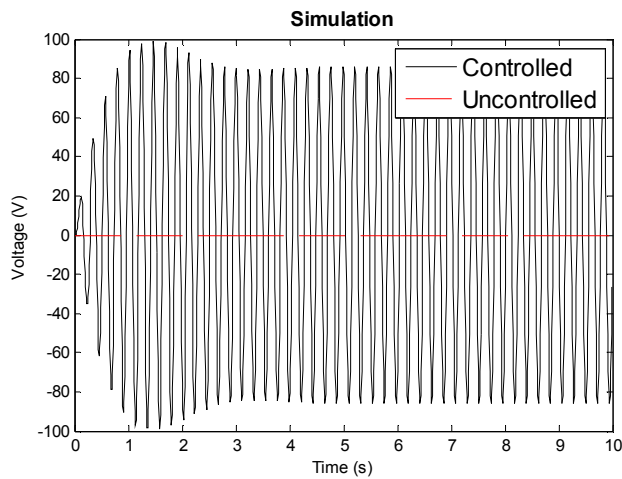


Figure 20 actuation voltages for one actuator damping.

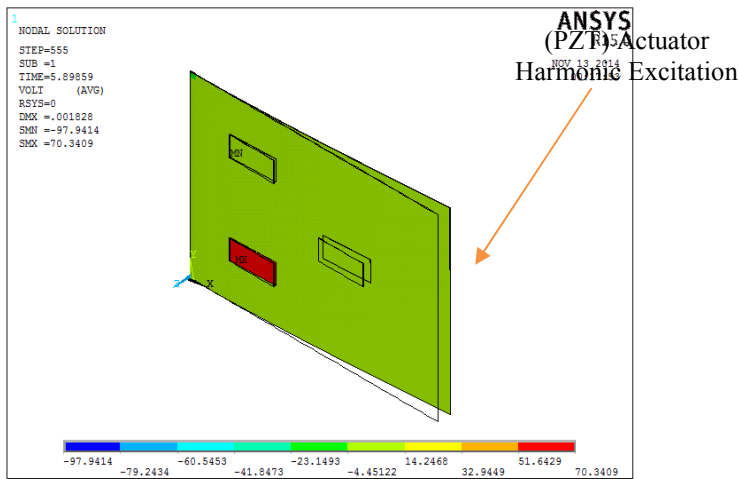


Figure 21 Actuation voltages contour for one Actuator damping (harmonic excitation)

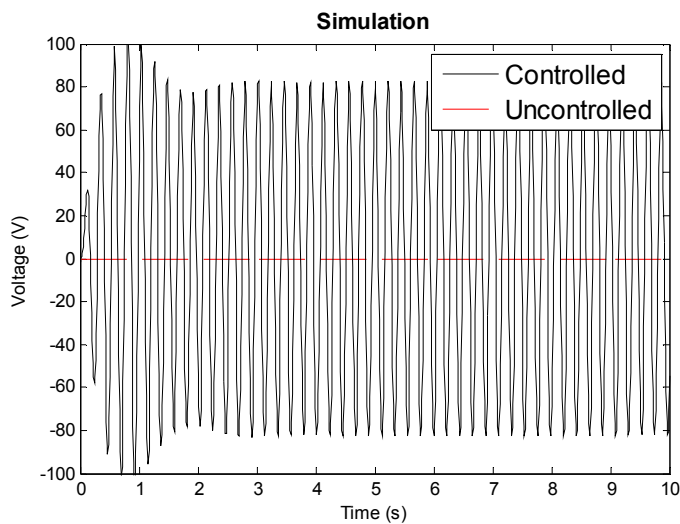


Figure 22 actuation voltages for two actuator damping

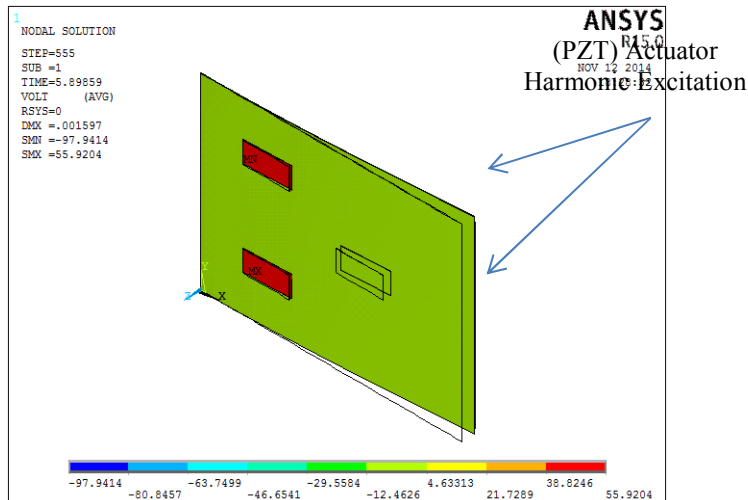


Figure 23 Actuation voltages contour feedback control for two Actuator damping (Harmonic Excitation)

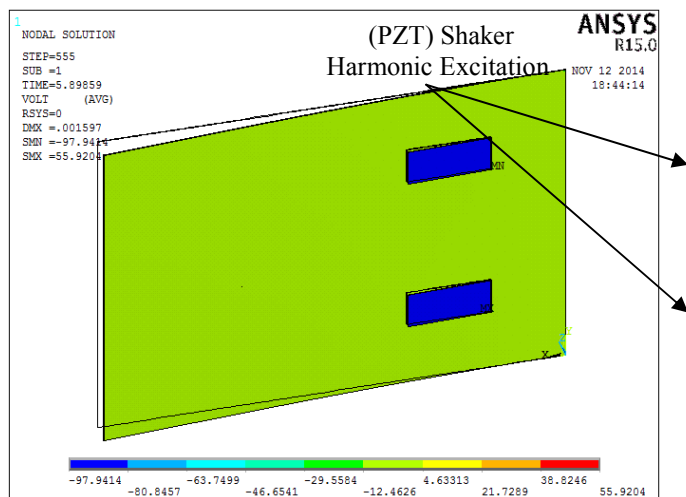


Figure 24 excitation smart plate by two PZT shakers

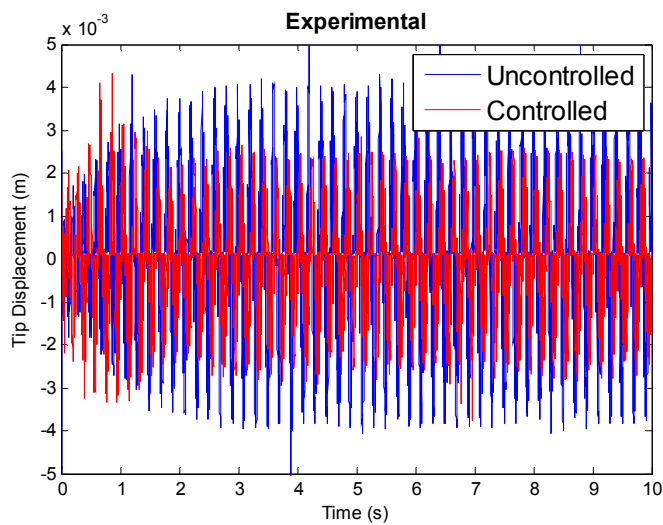


Figure 25 Uncontrolled and controlled vibration responses for one actuator damping $K_p=15$, (90-100)V for first mode

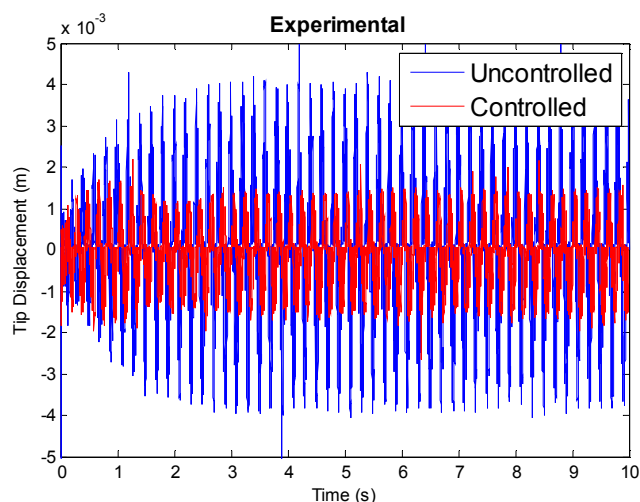


Figure 26 Uncontrolled and controlled vibration responses For two actuator damping, $K_p=15$, (90-100)V for first mode

9. Conclusions:

The main conclusions obtained from the present work can be summarized as follow:

It is found that in Active Vibrations Control under harmonic excitation, the controlled responses for two actuator damping provides better reduction in the amplitudes from one actuator damping. It is clear that there is a reduction of 46% for one actuator and 75% for two actuator reduction in steady-state vibration amplitudes for simulation while 39% and 67% in steady-state vibration amplitudes for experimental case..

This study not only solves the problem of theoretical arithmetic hardly solved of complex unit collocation, but also saves a lot of manpower and financial resources in experimental debugging. The experiment method and course presented in this study illustrates a good prospect of application and extension.

References

- [1] Khaled S, "Effect of piezoelectric actuator placement on controlling the modes of vibration for flexible structure", King Fahd University, Saudi Arabia, A Thesis in Master of Science, mechanical engineering, July 2005.
- [2] D.C. Hyland, J.L. Junkins, R.W. Longman, "Active control technology for large space structures", Journal of Guidance Control and Dynamics, Vol.16, pp. 801–821, 1993.
- [3] M.S. Kozien, J. Wiciak, Archives of Acoustics, Vol. 33, No. 4, pp. 643, 2008.
- [4] M. Kozupa and J. Wiciak "Active Vibration Control of Rectangular Plate with Distributed Piezoelements Excited Acoustically and Mechanically"/ University of Science and Technology AGH al. Mickiewicza Vol.3, pp.30-059 Kraków, Poland/2010.
- [5] T. A. Zahidi Rahman, I. Z. M. Darus. "Experimental Evaluation of Active Vibration Control of a Flexible Plate using Proportional Gain Controller". IEEE, 2011.
- [6] H.Karagu, L Malgaca and H .ktem. "Analysis of active vibration control in smart structures by ANSYS". Smart Materials and Structures Vol.13, pp.661–667, 2004.
- [7] ANSYS, 2004. ANSYS user manual, ANSYS, Inc., Canonsburg, PA, USA, (www.ansys.com).
- [8] T.H. Brockmann, *Theory of Adaptive Fiber Composites*, Solid Mechanics Springer Science Business Media B.V. 2009.
- [9] P. Gardonio, "Sensor-Actuator Transducers for Smart Panels", Australia 2006.
- [10] A. R. Tavakolpour, M. Mailah and I. Z. Mat Darus, "Active Vibration Control of a Rectangular Flexible Plate Structure Using High Gain Feedback Regulator," *International Review of Mechanical Engineering*, Vol. 3, No. 5, pp. 579-587, 2009.
- [11] Yaman, Caliskan, Nalbantoglu, Prasad, Waechter. "Active Vibration Control of a Smart Plate", ICAS CONGRESS 2002.
- [12] M. Yaqoob, N. Ahmad and M. Naushad. "Finite element analysis of actively controlled smart plate with patched actuators and sensors". Solids and Structures, Vol.7, pp. 227 – 247, 2010.
- [13] D.S. Bayard, F.Y. Hadaegh D.R Meldrum. "Optimal Experiment Design for identification of Large Space Structures". Automatica, 1998, Vol.24, No.3, pp.357-364.
- [14] X.Wang, J.Wang, Z.Gao and X.Zhu "Simulation and Experimental Study on Active Vibration Control of Piezoelectric Smart Plate Based on ANSYS" Shanghai, CHINA, IEEE 2010.

The IISTE is a pioneer in the Open-Access hosting service and academic event management. The aim of the firm is Accelerating Global Knowledge Sharing.

More information about the firm can be found on the homepage:

<http://www.iiste.org>

CALL FOR JOURNAL PAPERS

There are more than 30 peer-reviewed academic journals hosted under the hosting platform.

Prospective authors of journals can find the submission instruction on the following page: <http://www.iiste.org/journals/> All the journals articles are available online to the readers all over the world without financial, legal, or technical barriers other than those inseparable from gaining access to the internet itself. Paper version of the journals is also available upon request of readers and authors.

MORE RESOURCES

Book publication information: <http://www.iiste.org/book/>

Academic conference: <http://www.iiste.org/conference/upcoming-conferences-call-for-paper/>

IISTE Knowledge Sharing Partners

EBSCO, Index Copernicus, Ulrich's Periodicals Directory, JournalTOCS, PKP Open Archives Harvester, Bielefeld Academic Search Engine, Elektronische Zeitschriftenbibliothek EZB, Open J-Gate, OCLC WorldCat, Universe Digital Library, NewJour, Google Scholar

